Clinical Imaging 55 (2019) 65–70

Contents lists available at ScienceDirect

Clinical Imaging

journal homepage: www.elsevier.com/locate/clinimag

Imaging Physics and Informatics

Measurement of the liver iron concentration in transfusional iron overload by MRI R2* and by high-transition-temperature superconducting magnetic susceptometry

Sujit Sheth[a], Christopher J. Allen[b], David E. Farrell[c], John H. Tripp[c], Ramin Jafari[d], Yi Wang[a,d], Gary M. Brittenham[b,*]

[a] Weill Cornell Medical College, New York, NY, USA
[b] Columbia University Medical Center, New York, NY, USA
[c] Case Western Reserve University, Cleveland, OH, USA
[d] Cornell University, Ithaca, NY, USA

ARTICLE INFO

Keywords:
MRI
R2*
Magnetic susceptometry
Superconducting transition temperature
Liver iron concentration
High-transition-temperature superconductors

ABSTRACT

Purpose: To compare measurement of the liver iron concentration in patients with transfusional iron overload by magnetic resonance imaging (MRI), using R2*, and by magnetic susceptometry, using a new high-transitiontemperature (high-Tc; operating at 77 K, cooled by liquid nitrogen) superconducting magnetic susceptometer.

Methods: In 28 patients with transfusional iron overload, 43 measurements of the liver iron concentration were made by both R2* and high-Tc magnetic susceptometry.

Results: Measurements of the liver iron concentration by R2* and high-Tc magnetic susceptometry were significantly correlated when comparing all patients (Pearson's $r = 0.91$, $p < 0.0001$) and those with results by susceptometry > 7 mg Fe/g liver, dry weight ($r = 0.93$, $p = 0.006$). In lower ranges of liver iron, no significant correlations between the two methods were found (0 to < 3.2 mg Fe/g liver, dry weight: $r = 0.2$, $p = 0.37$; 3.2 to 7 mg Fe/g liver, dry weight: $r = 0.41$; $p = 0.14$).

Conclusion: The lack of linear correlation between R2* and magnetic susceptibility measurements of the liver iron concentration with minimal or modest iron overload may be due to the effects of fibrosis and other cellular pathology that interfere with R2* but do not appreciably alter magnetic susceptibility.

1. Introduction

Transfusional iron overload progressively develops in patients with refractory anemia who undergo regular red blood cell transfusion (thalassemia major, sickle-cell disease, myelodysplasia and other conditions) because the body lacks any effective means to excrete surplus iron [1]. Excess iron from transfused RBCs eventually leads to the formation of circulating non-transferrin-bound iron that is progressively deposited in the liver, pancreas, heart and other organs, causing fibrosis, cirrhosis, diabetes, heart failure, and other disorders [2–4]. Iron-chelating therapy can remove excess iron from cells, clear circulating non–transferrin-bound iron, and maintain or return body iron to safe levels. Safe iron-chelating therapy requires careful adjustment of the dose of iron-chelating agents to the body iron burden using the liver iron concentration [2,5–7] to optimize iron excretion while avoiding chelator toxicity, including gastrointestinal disorders, auditory and visual impairment, agranulocytosis and neutropenia, arthropathy, growth retardation, and potentially fatal hepatic failure, renal failure, and gastrointestinal hemorrhage [8–11].

As body iron accumulates in patients requiring chronic transfusion, the amounts of iron in functional and transport compartments undergo only minimal changes [12]; virtually all the excess iron is sequestered as paramagnetic ferritin and hemosiderin iron within macrophages of the liver, bone marrow and spleen. In an MR scanner, the magnetic field

Abbreviations: MRI, magnetic resonance imaging; LIC, liver iron concentration; T_c, superconducting transition temperature, i.e., the characteristic temperature of a material below which all electrical resistance is lost.; Low-Tc, low-transition-temperature (operating at 4 K, cooled by liquid helium); High-Tc, high-transition-temperature (operating at 77 K, cooled by liquid nitrogen)

* Corresponding author at: Columbia University Medical Center, Division of Pediatric Hematology, Oncology, and Stem Cell Transplantation, Children's Hospital North 10th Floor, Room 10-08, 3959 Broadway, New York, NY 10032, USA.
E-mail address: gmb31@columbia.edu (G.M. Brittenham).

https://doi.org/10.1016/j.clinimag.2019.01.012
Received 6 May 2018; Received in revised form 11 December 2018; Accepted 15 January 2019

of paramagnetic iron contributes to both transverse relaxation rates (R2) and intravoxel dephasing (R2′). R2* (=R2 + R2′) is readily measured by commercially available MRI pulse sequences to estimate the liver iron concentration [6]. Measurement of the transverse relaxation rate, R2* (=1/T2*), to estimate the liver iron concentration has become the most widely used magnetic resonance imaging (MRI) method to guide iron-chelating therapy in transfusional iron overload [6,13]. Still, the relationship between R2* and the liver iron concentration is complex, in part because intravoxel contents other than iron contribute to relaxation [14].

A noninvasive alternative is to measure the liver iron by magnetic susceptometry. In contrast to R2*, the change in the magnetic susceptibility of a tissue has a direct biophysical connection and linear relationship to the tissue iron concentration. Such noninvasive comparisons with R2* have been reported for a room-temperature magnetic iron detector measuring whole-body susceptibility [15] and for a low-transition-temperature (low-T_c; operating at 4 K, cooled by liquid helium) biomagnetic susceptometer using superconducting quantum interference device (SQUID) amplifiers to measure liver susceptibility [16]. In superconductivity, the transition temperature (T_c) is the characteristic temperature of a material below which all electrical resistance is lost. We have developed a new improved method to measure the magnetic susceptibility of liver using high-transition-temperature (high-Tc; operating at 77 K, cooled by liquid nitrogen) superconductors [17,18]. We report here a retrospective comparison of determination of the liver iron concentration by clinical MRI measurement of R2* and by high-T*c* magnetic susceptometry.

2. Material and methods

2.1. Patient selection

We retrospectively examined the records of high-T*c* magnetic susceptibility measurements and of R2* determinations made within 4 months of each other in conjunction with annual assessments of iron-chelating therapy in patients with transfusional iron. As in a related study [16], no significant differences in the liver iron concentration were expected between R2* and magnetic susceptibility studies during the 4 month interval. The participation of human subjects was approved by the Institutional Review Boards. Written informed consent was provided by participants, parents, and guardians, along with written informed assent when applicable.

2.2. High-transition temperature (high-Tc) susceptometer measurements

The instrumentation for these studies has been described in detail elsewhere [17,18] and the components of the high-T*c* susceptometer are shown in Fig. 1. In brief, the high-T*c* susceptometer has redesigned and replaced each of the three elements which utilize superconductivity in liquid-helium-cooled low-T*c* susceptometers [19,20]. First, detectors and flux transformers patterned from high-homogeneity high-transition-temperature superconducting tape replace the detection coils and flux transformer of the low-T*c* device. Second, high-strength rare-earth Neodymium-Boron-Iron (NdBFe) permanent magnets take the place of low-T*c* field coils to produce a steady localized magnetic field over the right lobe of the liver [17]. Third, magnetoresistive sensors housed in Mu-metal shielding cylinders are used instead of low-T*c* SQUID amplifiers [17,18]. The complete high-T*c* susceptometer utilizes two magnets and five independent flux-sensing channels. Two of the sensing channels detect the spatial variation of the signal above the subject and the remaining three are used for noise cancelation. The design and geometry of the magnets and detector coils aimed to optimize the ability of the instrument to correct for the presence of non-hepatic tissue beneath the detector coils by distinguishing and separating its contribution from that of the liver. The calibration of the high-T*c* susceptometer is described in detail elsewhere [17]. In sum, compared to low-T*c* instruments, these alterations have increased the signal from the liver by fifty-fold and offer the operational advantage of using liquid nitrogen rather than liquid helium to cool the superconducting components.

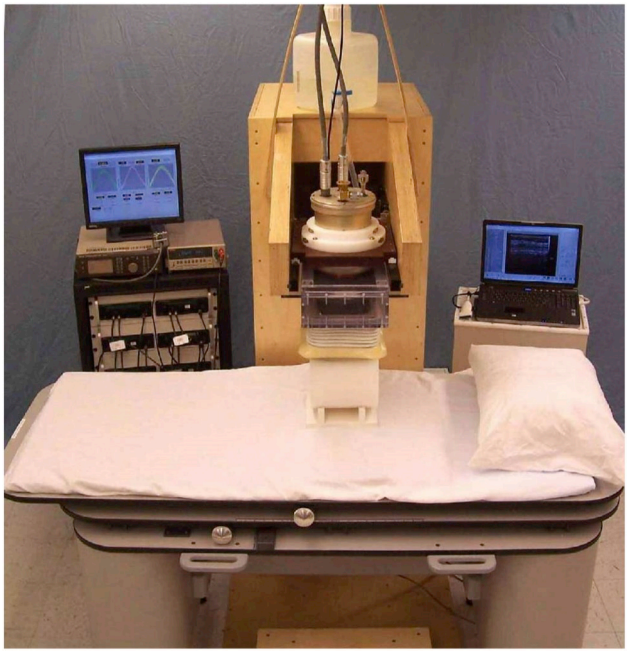

Fig. 1. The new high-transition-temperature (high-Tc; operating at 77 K, cooled by liquid nitrogen) superconducting magnetic susceptometer, set up to measure the susceptibility of a solid polyethylene cylinder with respect to water. The principal components of the system are the support bed (front), data acquisition electronics (left rear), susceptometer module, polyethylene cylinder and water bellows (center), and support gantry (center, rear).

For a liver iron measurement, initially an ultrasound scan is made to determine the location and depth of the liver beneath the skin surface. The patient is then positioned beneath the susceptometer module with the point where the ultrasound depth measurement was made centered beneath the susceptometer coils. The water bellows is filled and the support bed raised until the patient is at a minimal distance from the center of the susceptometer coils. The susceptometer module is then set in lateral motion for a series of transverse periodic scans of the liver. A single liver iron determination was made from the mean of six transverse scans over the liver. Each transverse scan required about 1 min and consisted of a total of 15 cycles of susceptometer motion. Generally, to assess reproducibility, the patient was repositioned beneath the susceptometer and a duplicate liver iron determination was made. Using custom software, the volume magnetic susceptibility of the liver, χ_c, is calculated in real time from the experimental susceptibility scans [24], and the liver iron concentration (LIC) obtained using the ferritin/hemosiderin specific mass susceptibility [21,22]

$$X = 1.6{\cdot}10^{-6} m^3/Kg_{Fe};\ \mathrm{LIC} = \chi_c/X.$$

2.3. MRI measurements

MRI measurements were made using a 1.5 T MRI scanner (General Electric SignaHDx 15.0, Waukesha, WI) using an 8-channel phased array cardiac coil centered over the liver. A total of 2–4 slices was acquired using a breath-hold multi-echo 2D GRE sequence with the following imaging parameters: number of echoes = 16, flip angle = 20°, TE_1 = 0.9 msec, ΔTE = 1 msec, TR = 25 msec, voxel size = 1.9 × 1.9 × 10 mm3, BW = 976 Hz/pixel, matrix size = 256 × 256. The magnitude of GRE echoes was incorporated for liver R2* measurement using GE ReportCard StarMap 4.0 software with the radiologist drawing ROIs on the liver while avoiding

vessels and inhomogeneous regions. LIC was obtained from R2* values using the equation [23]:

$$[LIC]R2^* = 0.0254 \times R2^* + 0.202.$$

2.4. Statistical analysis

The linear relationships between R2* and high-Tc magnetic susceptibility measurements of the liver iron concentration were assessed using Pearson's coefficient of correlation and linear regression analysis. Bland-Altman plots were used to estimate the bias and 95% limits of agreement between the two methods [24]. The Prism 7.0d (GraphPad Software. La Jolla, CA) statistical computer package was used for computations. All statistical tests were two-tailed and a significance level of 0.05 was used.

3. Results

3.1. Study population

Between 2011 and 2015,180 high-Tc measurements were made in 51 patients with various forms of iron overload in our laboratory in New York, NY. Of these, a total of 43 magnetic susceptibility measurements were made within 4 months of clinical R2* studies conducted in conjunction with annual assessments of iron-chelating therapy in 28 patients, 5 to 48 years of age. The indications for transfusion in these patients were thalassemia major ($n = 20$), thalassemia intermedia ($n = 3$), hemoglobin E – beta thalassemia ($n = 1$), Diamond-Blackfan anemia (n = 1), pyruvate kinase deficiency (n = 1), hereditary elliptocytosis (n = 1), and congenital erythropoietic porphyria (n = 1).

3.2. Comparison of MRI R2* and high-Tc susceptometric determinations of the liver iron concentration

The results of the R2* and high-Tc determinations of the liver iron concentration in the patients with transfusional iron overload are summarized in Fig. 2, showing graphically the correlations observed and the limits of agreement between the two methods. For each group of patients, the Supplemental Table provides the linear regression equations with 95% confidence intervals for the slope and the x and y intercepts, the Pearson correlation coefficients with 95% confidence intervals, and the Bland-Altman estimates of bias and the 95% limits of agreement. The standard deviations of duplicate susceptometric measurements of liver iron ranged from 0.2 to 0.9 mg Fe/g liver, dry weight (dw). The standard deviations of the R2* measurements of liver iron were not included in the clinical reports, but typically would range from 0.2 to about 5 mg Fe/g liver, dw, for this range of liver iron concentrations. Overall, measurements of the liver iron concentration by R2* and high-Tc magnetic susceptometry were significantly correlated when comparing all patients: Pearson's $r = 0.91$, 95% confidence interval, 0.84 to 0.95, $p < 0.0001$). Bland-Altman analysis found a bias of 47.1% ± 51.1% (SD), with wide 95% limits of agreement from −53.1% to 147.3%. Further analysis was then carried out using thresholds widely used to guide iron-chelating therapy in the absence of cardiac iron overload: < 3.2 mg Fe/g liver, dw: increased risk of chelator-related complications; 3.2 to < 7 mg Fe/g liver, dw: optimal range for safe storage of transfused iron; 7 to < 15 mg Fe/g liver, dw: increased risk of iron-related complications; > 15 mg Fe/g liver, dw: greatly increased risk of cardiac disease and early death [2,5–7].

For patients with results by susceptometry > 7 mg Fe/g liver, dry weight, measurements of the liver iron concentration by R2* and high-Tc magnetic susceptometry were significantly correlated, Pearson's $r = 0.93$, 95% confidence interval, 0.52 to 0.99, $p = 0.006$, with a bias of 36.7% (± 27.3%) and 95% limits of agreement from −16.8% to 90.2%. By contrast, at lower liver iron concentrations, as determined by susceptometry, correlations between the two methods of measurement were no longer significant. For the optimal range of 3.2 to < 7 mg Fe/g liver, dw, the value of Pearson's r was 0.42, 95% confidence interval, −0.15 to 0.78, $p = 0.14$, with a bias of 39.7% (± 40.9.3%) and 95% limits of agreement from −40.5% to 119.9%. For the range indicating an increased risk of chelator-related complications, < 3.2 mg Fe/g liver, dry weight, $r = 0.20$, 95% confidence interval, −0.23 to 0.56, $p = 0.37$, with a bias of 54.3% (± 60.9%) and 95% limits of agreement from –65.1% to 173.8%. Fig. 2 illustrates graphically the correlations observed and the wide limits of agreement between the two methods.

4. Discussion

Our results demonstrate that the correlation between the liver iron concentration (LIC) estimated by MRI R2* and that determined by our new noninvasive high-Tc magnetic susceptometer is significant over a large LIC range (from 0 to 25 mg Fe/g liver dw), but no longer significant either within the optimal range for safe storage of transfused iron (from 3.2 to 7 mg Fe/g liver dw) or within the range for an increased risk of chelator-related complications (from 0 to 3.2 mg Fe/g liver dw). With greater iron burdens, the contributions to R2* of marked and severe iron overload become dominant, resulting in the observed linear correlations between R2* and susceptometric results over the entire extent of LIC examined in our study. In contrast, with lesser iron burdens, those < 7 mg Fe/g liver dw, the linear relationship between R2* and susceptometry is no longer significant, suggesting a need for careful examination of the accuracy of noninvasive measures in these lower, more restricted but clinically important ranges of LIC.

Overall, our data had lower variability but were consistent with those from two previous reports comparing R2* with noninvasive magnetic measurements; these earlier studies also identified a lack of correlation between the methods at lower LIC. In 97 patients with iron overload, a correlation of $r = 0.82$ was found using a room-temperature magnetic iron detector [15]. This magnetic iron detector estimates the total amount of iron in the liver by measuring the susceptibility of the whole human body. Using a model based on a three-dimensional shape of the patient acquired with a laser scan system, the total iron in the liver is then derived and the liver iron concentration calculated by dividing the total iron by the liver volume [15]. In studies of 14 patients with iron overload using a liquid-helium-cooled low-Tc magnetic susceptometer conducted in Hamburg, Germany, a somewhat stronger overall correlation, $r = 0.92$, was found with R2*; an additional 8 patients could not be studied because of unreliable estimates of R2* [16]. Neither of these earlier studies examining R2* and magnetic susceptibility estimates examined the relationship between the two methods at lower liver iron concentrations. Inspection of the plots of the results of the earlier magnetic susceptibility studies suggests a similar lack of significant correlation at lower iron concentrations (Cf. Fig. 3b in Gianesin et al., 2012 [15]; Fig. 3 in Sharma et al., 2017 [16]). Furthermore, several investigators have compared R2* with the reference method for measurement of the liver iron concentration [25], chemical measurement of the iron concentration in a liver-biopsy specimen obtained by percutaneous biopsy [26–31]. Prior studies comparing R2* and liver biopsy results have found significant correlations over a wide range of liver iron concentrations but have not specifically examined the range < 7.0 mg/g liver, dw [26–34]. Still, plots of these results show considerable scatter and suggest unacceptably broad limits of agreement [14,33,35]. In contrast, the concentration of iron in liver tissue and that measured by magnetic susceptometry are linearly related below 7.0 mg/g liver. dw [36]. The lack of quantitative connection between R2* and lower LICs is caused primarily by relaxation interference by intravoxel contents, especially by hepatic fibrosis, which is present in up to 90% or more of patients with transfusional iron overload [14]. Free water protons that generate the MRI signal experience relaxation caused by proton spin-spin interactions that are highly dependent on the microenvironment of cellular contents, including the presence of macromolecular fibrosis. Water diffusion in the

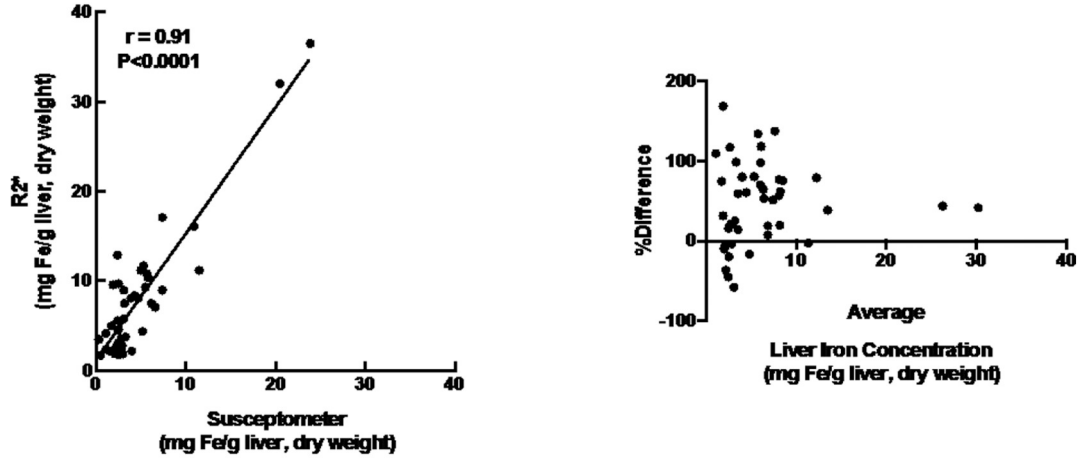

A. All patients

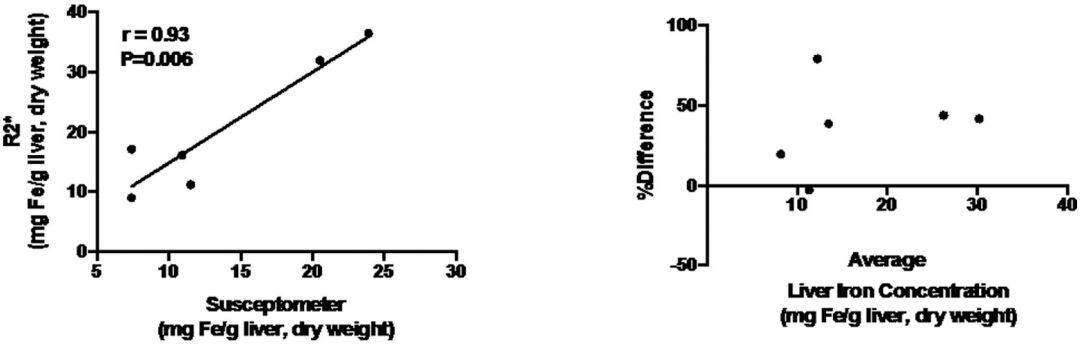

B. Susceptometer LIC > 7 mg Fe/g dry weight

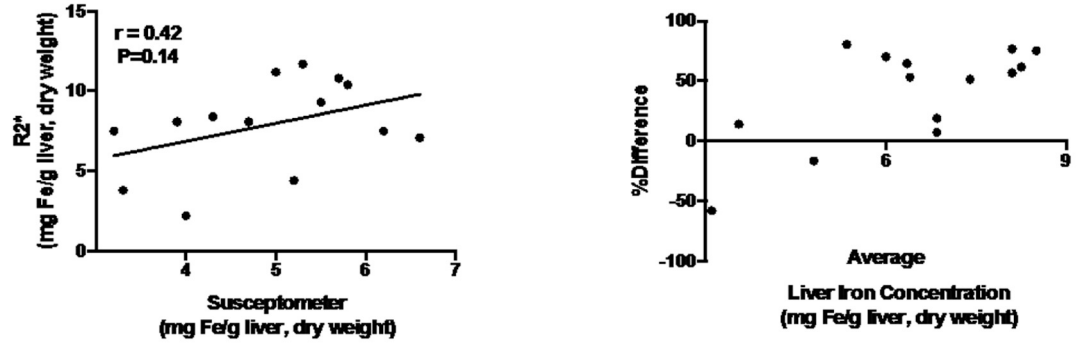

C. Susceptometer LIC > 3.2 - 7 mg Fe/g dry weight

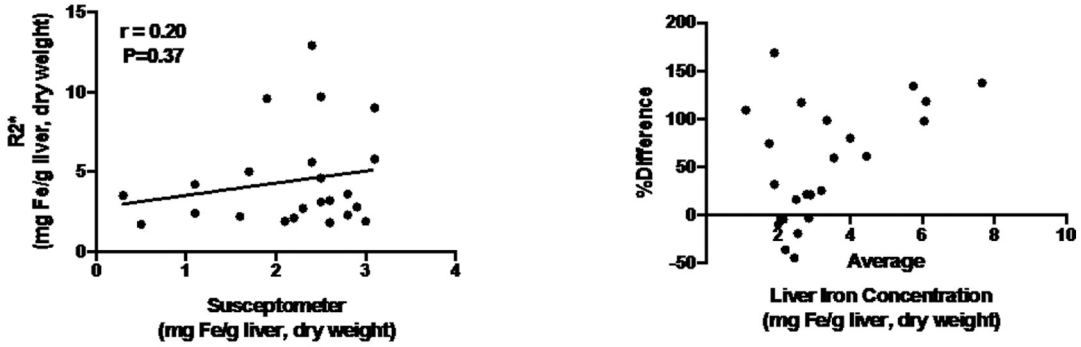

D. Susceptometer LIC < 3.2 mg Fe/g dry weight

(caption on next page)

Fig. 2. Relationships between liver iron concentration (LIC) determined by MRI R2* and by high-transition-temperature (high-Tc; operating at 77 K, cooled by liquid nitrogen) magnetic susceptometry (left panels), and Bland-Altman plots of the percent difference between the R2* and susceptometric measurements and their average (right panels). A. All patients. B. Patients with LIC by susceptometry > 7 mg Fe/g dry weight C. Patients with LIC by susceptometry > 3.2–7 mg Fe/g dry weight. D. Patients with LIC by susceptometry 0 to 3.2 mg Fe/g dry weight.

inhomogeneous field of the paramagnetic iron also causes signal decay as modeled by field correlation [37]. Additionally, water exchange among sites also causes signal decay (19). The R2* decay rate of the MRI signal depends in a complex nonlinear fashion on both the iron distribution and the cellular microenvironment of water. In the absence of any direct biophysical connection between R2* and the liver iron concentration, empirical approaches have been used for the conversion of an R2* value, in Hertz (Hz), into a liver iron concentration, expressed in milligrams or micromoles of iron per gram liver, dry weight (mg Fe or μmol/g liver, dw).

Interference from fibrosis is minimal in magnetic susceptibility measurements because weakly diamagnetic fibrosis has little effect on susceptibility. Using our original low-Tc susceptometer, the correlation between the hepatic iron concentration as determined by magnetic susceptometry and by chemical analysis of liver tissue obtained by clinically indicated biopsy was $r = 0.99$ in 48 patients with transfusional iron overload [36]; patients with cirrhosis and those with biopsy specimens < 5 mg, wet weight, were excluded. In 25 patients with transfusional iron overload, concurrent high-Tc and low-Tc susceptometric measurements of the liver iron had a correlation of $r = 0.98$. In the present study, while technical features of both the MRI and magnetic susceptibility measurements undoubtedly accounted for some of the discordance between the two methods, the interfering effects of fibrosis and other cellular pathology on R2* but not on magnetic susceptibility are likely to have been major contributors. In addition, recent studies in vitro of liver samples concluded that “MRI methods based on T1 or T2 measurements will not provide an accurate quantification of tissue iron content at low iron concentrations” [38], citing the effects of iron loading (the number of iron ions per ferritin molecule), the microscopic distribution of iron in tissue, and the relative proportions of ferritin and hemosiderin iron.

Magnetic susceptibility of the liver can also be determined using MRI quantitative susceptibility mapping (QSM) [39]. The field measurements at all voxels in QSM are much more numerous that the susceptometer field measurements, suggesting QSM is more accurate than susceptometer. QSM identifies the magnetic field induced by tissue from MRI signal phase [40] and deconvolves the field to determine tissue susceptibility [41], overcoming the blooming artifacts in R2* [42]. The same multi-echo gradient-echo data that are used to derive R2* from the magnitude data can be used to derive QSM [16,41,43]. QSM has been demonstrated to be more sensitive than R2* in detecting nigral iron overload in Parkinson's disease [44,45]. As in the present study, our prior study of patients with liver iron overload using QSM found a significant correlation overall ($r = 0.89$) but no significant correlation in those with lower iron burdens [14]. Phantom studies demonstrated collagen interference with R2* but not with QSM [14]. Altogether, these results provided evidence that intravoxel contents other than iron, including fibrosis and necroinflammation, alter R2* but marginally affect measurements of magnetic susceptibility [14]. Hepatic fibrosis, reported in from 50 to > 90% of patients with transfusional iron overload [29,31,46], seems a likely cause of much of the discrepancy between R2* and magnetic susceptibility measurements seen with minimal or modest iron overload [14].

The results presented here have implications for clinical practice. The usefulness of a method that can only provide accurate measurements at high liver iron concentrations is limited. Caution is needed, especially in patients with minimal or modest iron overload (liver iron concentration < 7 mg Fe/g liver, dw), because fibrosis and other cellular pathology can interfere with and limit the accuracy of R2* measurements of liver iron overload. For these patients, a major concern is over chelation. Chelator toxicity depends upon the agent used but includes i) ocular and auditory disturbances, growth retardation and skeletal changes, respiratory distress syndrome (deferoxamine), ii) agranulocytosis and neutropenia; gastrointestinal disturbances, arthropathy, increased liver-enzyme levels and progression of hepatic fibrosis (deferiprone), and iii) gastrointestinal disturbances, rash, and renal abnormalities (deferasirox) (4, 37, 38). After initial approval of deferasirox, the FDA later required the addition of a “black-box” warning of potentially fatal chelator toxicity from renal failure, hepatic failure and gastrointestinal hemorrhage. Although the mechanisms of these serious and other adverse effects are not well understood and some reactions may be idiosyncratic, the risks generally are considered to be increased if the amounts of iron chelator administered exceed the amounts of storage iron available for chelation. If fibrosis or other factors lead to R2* overestimation of the liver iron, the risk of over chelation increases. Finally, these results question suggestions that “Liver MRI is more precise than liver biopsy for assessing total body iron balance” [47].

Our study is limited by the lack of comparisons with the reference standard, chemical measurements of liver-biopsy specimens [25]. In our current practice, percutaneous biopsies for LIC assessment in thalassemia are infrequent, in part because of the risk of complications, discomfort, and lack of acceptability to patients. Patients undergoing liver transplantation may be recruited for studies to validate non-invasive methods for measuring LIC.

5. Conclusion

The lack of linear correlation between R2* and magnetic susceptibility measurements of the liver iron concentration with minimal or modest iron overload may be due to the effects of fibrosis and other cellular pathology that interfere with R2* but do not appreciably alter magnetic susceptibility. The influence of other factors remains to be determined, such as iron loading of ferritin, the microscopic distribution of iron in tissue, and the relative proportions of ferritin and hemosiderin iron.

Supplementary data to this article can be found online at https://doi.org/10.1016/j.clinimag.2019.01.012.

Declarations of interest

None.

Acknowledgements

This work was supported in part by the U.S. Food and Drug Administration (FDA) Orphan Products Program, through Grant Number R01 FD003702, in part by NIH Grants R01 DK116126, R01 NS095562, UL1RR024156, and UL1TR000040, and in part by the National Center for Advancing Translational Sciences, National Institutes of Health (NIH), through Grant Number UL1TR001873. The content is solely the responsibility of the authors and does not necessarily represent the official views of the U.S. Food and Drug Administration or the National Institutes of Health.

References

[1] Brittenham GM. Disorders of iron homeostasis: iron deficiency and overload. In: Hoffman RBE, Silberstein LE, Heslop H, Weitz JI, Anastasi J, Salama ME, Abutalib SA, editors. Hematology: Basic Principles and Practice. New York: Elsevier; 2018. p. 478–90.

[2] Brittenham GM. Iron-chelating therapy for transfusional iron overload. N Engl J Med 2011;364(2):146–56.
[3] Coates TD. Physiology and pathophysiology of iron in hemoglobin-associated diseases. Free Radic Biol Med 2014;72:23–40.
[4] Porter JB, de Witte T, Cappellini MD, Gattermann N. New insights into transfusion-related iron toxicity: implications for the oncologist. Crit Rev Oncol Hematol 2016;99:261–71.
[5] Hoffbrand AV, Taher A, Cappellini MD. How I treat transfusional iron overload. Blood 2012;120(18):3657–69.
[6] Labranche R, Gilbert G, Cerny M, Vu KN, Soulieres D, Olivie D, et al. Liver Iron quantification with MR imaging: a primer for radiologists. Radiographics 2018;38(2):392–412.
[7] Olivieri NF, Brittenham GM. Management of the thalassemias. Cold Spring Harb Perspect Med 2013;3(6).
[8] Botzenhardt S, Li N, Chan EW, Sing CW, Wong IC, Neubert A. Safety profiles of iron chelators in young patients with haemoglobinopathies. Eur J Haematol 2017;98(3):198–217.
[9] Diaz-Garcia JD, Gallegos-Villalobos A, Gonzalez-Espinoza L, Sanchez-Nino MD, Villarrubia J, Ortiz A. Deferasirox nephrotoxicity-the knowns and unknowns. Nat Rev Nephrol 2014;10(10):574–86.
[10] Martin-Sanchez D, Gallegos-Villalobos A, Fontecha-Barriuso M, Carrasco S, Sanchez-Nino MD, Lopez-Hernandez FJ, et al. Deferasirox-induced iron depletion promotes BclxL downregulation and death of proximal tubular cells. Sci Rep 2017;7:41510.
[11] Ramaswami A, Rosen DJ, Chu J, Wistinghausen B, Arnon R. Fulminant liver failure in a child with beta-thalassemia on deferasirox: a case report. J Pediatr Hematol Oncol 2016;39:235–7.
[12] Brittenham GM, Badman DG. National Institute of D, digestive, kidney diseases W. Noninvasive measurement of iron: report of an NIDDK workshop. Blood 2003;101(1):15–9.
[13] Wood JC. Estimating tissue iron burden: current status and future prospects. Br J Haematol 2015;170(1):15–28.
[14] Li J, Lin H, Liu T, Zhang Z, Prince MR, Gillen K, et al. Quantitative susceptibility mapping (QSM) minimizes interference from cellular pathology in R2* estimation of liver iron concentration. J Magn Reson Imaging 2018;48:1069–79.
[15] Gianesin B, Zefiro D, Musso M, Rosa A, Bruzzone C, Balocco M, et al. Measurement of liver iron overload: noninvasive calibration of MRI-R2* by magnetic iron detector susceptometer. Magn Reson Med 2012;67(6):1782–6.
[16] Sharma SD, Fischer R, Schoennagel BP, Nielsen P, Kooijman H, Yamamura J, et al. MRI-based quantitative susceptibility mapping (QSM) and R2* mapping of liver iron overload: comparison with SQUID-based biomagnetic liver susceptometry. Magn Reson Med 2017;78(1):264–70.
[17] Farrell DE, Allen CJ, Whilden MW, Kidane TK, Baig TN, Tripp JH, et al. A new instrument designed to measure the magnetic susceptibility of human liver tissue in vivo. IEEE Trans Magn 2007;43(9):3543–54.
[18] Farrell DE, Allen CJ, Whilden MW, Tripp JH, Usoskin A, Sheth S, et al. Magnetic measurement of liver iron stores: engineering aspects of a new scanning susceptometer based on high-temperature superconductivity. IEEE Trans Magn 2007;43(11):4030–6.
[19] Brittenham GM, Farrell DE, Harris JW, Feldman ES, Danish EH, Muir WA, et al. Magnetic-susceptibility measurement of human iron stores. N Engl J Med 1982;307(27):1671–5.
[20] Fischer R, Harmatz PR. Non-invasive assessment of tissue iron overload. Hematology Am Soc Hematol Educ Program 2009:215–21.
[21] Bauman JH, Harris JW. Estimation of hepatic iron stores by vivo measurement of magnetic susceptibility. J Lab Clin Med 1967;70(2):246–57.
[22] Shoden A, Sturgeon P. Hemosiderin. Acta Haematol 1960;23(6):376–92.
[23] Meloni A, Rienhoff Jr. HY, Jones A, Pepe A, Lombardi M, Wood JC. The use of appropriate calibration curves corrects for systematic differences in liver R2* values measured using different software packages. Br J Haematol 2013;161(6):888–91.
[24] Bland JM, Altman DG. Measuring agreement in method comparison studies. Stat Methods Med Res 1999;8(2):135–60.
[25] Brittenham GM. Reference method for measurement of the hepatic iron concentration. Am J Hematol 2015;90(2):85–6.
[26] d'Assignies G, Paisant A, Bardou-Jacquet E, Boulic A, Bannier E, Laine F, et al. Noninvasive measurement of liver iron concentration using 3-Tesla magnetic resonance imaging: validation against biopsy. Eur Radiol 2018;28(5):2022–30.
[27] Gandon Y, Olivie D, Guyader D, Aube C, Oberti F, Sebille V, et al. Non-invasive assessment of hepatic iron stores by MRI. Lancet 2004;363(9406):357–62.
[28] Garbowski MW, Carpenter JP, Smith G, Roughton M, Alam MH, He T, et al. Biopsy-based calibration of T2* magnetic resonance for estimation of liver iron concentration and comparison with R2 Ferriscan. J Cardiovasc Magn Reson 2014;16:40.
[29] Hankins JS, McCarville MB, Loeffler RB, Smeltzer MP, Onciu M, Hoffer FA, et al. R2* magnetic resonance imaging of the liver in patients with iron overload. Blood 2009;113(20):4853–5.
[30] McCarville MB, Hillenbrand CM, Loeffler RB, Smeltzer MP, Song R, Li CS, et al. Comparison of whole liver and small region-of-interest measurements of MRI liver R2* in children with iron overload. Pediatr Radiol 2010;40(8):1360–7.
[31] Wood JC, Enriquez C, Ghugre N, Tyzka JM, Carson S, Nelson MD, et al. MRI R2 and R2* mapping accurately estimates hepatic iron concentration in transfusion-dependent thalassemia and sickle cell disease patients. Blood 2005;106(4):1460–5.
[32] Christoforidis A, Perifanis V, Spanos G, Vlachaki E, Economou M, Tsatra I, et al. MRI assessment of liver iron content in thalassamic patients with three different protocols: comparisons and correlations. Eur J Haematol 2009;82(5):388–92.
[33] Henninger B, Zoller H, Rauch S, Finkenstedt A, Schocke M, Jaschke W, et al. R2* relaxometry for the quantification of hepatic iron overload: biopsy-based calibration and comparison with the literature. RöFo 2015;187(6):472–9.
[34] Virtanen JM, Komu ME, Parkkola RK. Quantitative liver iron measurement by magnetic resonance imaging: in vitro and in vivo assessment of the liver to muscle signal intensity and the R2* methods. Magn Reson Imaging 2008;26(8):1175–82.
[35] St Pierre TG, Clark PR, Chua-anusorn W, Fleming AJ, Jeffrey GP, Olynyk JK, et al. Noninvasive measurement and imaging of liver iron concentrations using proton magnetic resonance. Blood 2005;105(2):855–61.
[36] Brittenham GM, Sheth S, Allen CJ, Farrell DE. Noninvasive methods for quantitative assessment of transfusional iron overload in sickle cell disease. Semin Hematol 2001;38(1 Suppl 1):37–56.
[37] Jensen JH, Chandra R. Strong field behavior of the NMR signal from magnetically heterogeneous tissues. Magn Reson Med 2000;43(2):226–36.
[38] Hocq A, Luhmer M, Saussez S, Louryan S, Gillis P, Gossuin Y. Effect of magnetic field and iron content on NMR proton relaxation of liver, spleen and brain tissues. Contrast Media Mol Imaging 2015;10(2):144–52.
[39] de Rochefort L, Liu T, Kressler B, Liu J, Spincemaille P, Lebon V, et al. Quantitative susceptibility map reconstruction from MR phase data using Bayesian regularization: validation and application to brain imaging. Magn Reson Med 2010;63(1):194–206.
[40] Zhou D, Liu T, Spincemaille P, Wang Y. Background field removal by solving the Laplacian boundary value problem. NMR Biomed 2014;27(3):312–9.
[41] Wang Y, Liu T. Quantitative susceptibility mapping (QSM): decoding MRI data for a tissue magnetic biomarker. Magn Reson Med 2015;73(1):82–101.
[42] Li J, Chang S, Liu T, Wang Q, Cui D, Chen X, et al. Reducing the object orientation dependence of susceptibility effects in gradient echo MRI through quantitative susceptibility mapping. Magn Reson Med 2012;68(5):1563–9.
[43] Wang Y, Spincemaille P, Liu Z, Dimov A, Deh K, Li J, et al. Clinical quantitative susceptibility mapping (QSM): biometal imaging and its emerging roles in patient care. J Magn Reson Imaging 2017;46(4):951–71.
[44] Du G, Liu T, Lewis MM, Kong L, Wang Y, Connor J, et al. Quantitative susceptibility mapping of the midbrain in Parkinson's disease. Mov Disord 2016;31(3):317–24.
[45] Barbosa JH, Santos AC, Tumas V, Liu M, Zheng W, Haacke EM, et al. Quantifying brain iron deposition in patients with Parkinson's disease using quantitative susceptibility mapping, R2 and R2. Magn Reson Imaging 2015;33(5):559–65.
[46] St Pierre TG, El-Beshlawy A, Elalfy M, Al Jefri A, Al Zir K, Daar S, et al. Multicenter validation of spin-density projection-assisted R2-MRI for the noninvasive measurement of liver iron concentration. Magn Reson Med 2014;71(6):2215–23.
[47] Wood JC, Zhang P, Rienhoff H, Abi-Saab W, Neufeld EJ. Liver MRI is more precise than liver biopsy for assessing total body iron balance: a comparison of MRI relaxometry with simulated liver biopsy results. Magn Reson Imaging 2015;33(6):761–7.